Biochemical and Biophysical Research Communications 424 (2012) 94–99

Contents lists available at SciVerse ScienceDirect

Biochemical and Biophysical Research Communications

journal homepage: www.elsevier.com/locate/ybbrc

Role of nesprin-1 in nuclear deformation in endothelial cells under static and uniaxial stretching conditions

Toshiro Anno [a], Naoya Sakamoto [b,*,1], Masaaki Sato [a]

[a] Department of Biomedical Engineering, Graduate School of Biomedical Engineering, Tohoku University, Sendai, Japan
[b] Department of Bioengineering and Robotics, Graduate School of Engineering, Tohoku University, Sendai, Japan

ARTICLE INFO

Article history:
Received 18 June 2012
Available online 21 June 2012

Keywords:
Nesprin-1
LINC complex
Nucleus
Force transmission
Endothelial cells

ABSTRACT

The linker of nucleus and cytoskeleton (LINC) complex, including nesprin-1, has been suggested to be crucial for many biological processes. Previous studies have shown that mutations in nesprin-1 cause abnormal cellular functions and diseases, possibly because of insufficient force transmission to the nucleus through actin filaments (F-actin) bound to nesprin-1. However, little is known regarding the mechanical interaction between the nucleus and F-actin through nesprin-1. In this study, we examined nuclear deformation behavior in nesprin-1 knocked-down endothelial cells (ECs) subjected to uniaxial stretching by evaluating nuclear strain from lateral cross-sectional images. The widths of nuclei in nesprin-1 knocked-down ECs were smaller than those in wild-type cells. In addition, nuclear strain in nesprin-1 knocked-down cells, which is considered to be compressed by the actin cortical layer, increased compared with that in wild-type cells under stretching condition. These results indicate that nesprin-1 knockdown releases the nucleus from the tension of F-actin bound to the nucleus, thereby increasing allowance for deformation before stretching, and that F-actin bound to the nucleus through nesprin-1 causes sustainable force transmission to the nucleus.

1. Introduction

Adherent cells such as endothelial cells (ECs) generate forces on their own through cytoskeletal actin filaments (F-actin) and interact with the extracellular matrix (ECM) or neighboring cells. This interaction is important for various cell functions and tissue development. F-actin connects adherens junctions (AJs) and focal adhesions (FAs) to each other, resulting in force application to adhesion molecules [1,2]. Intracellular force transmission is critical for a number of biological processes such as cell migration [3] and mitosis [4]. In addition to AJs and FAs, the nucleus has recently been reported to be connected to cytoskeletal F-actin. Such a nucleo-cytoskeletal connection is mediated by a protein complex consisting of nesprin, SUN, and lamin proteins, referred to as the linker of nucleus and cytoskeleton (LINC) complex [5]. Until date, four types of nesprins have been identified: nesprin-1, -2, -3, and -4. Nesprin-1 and -2 are reported to bind to F-actin through the N-terminus and to transmembrane SUN proteins, SUN1/2, through the C-terminus [6,7]. SUN1/2 bind to nuclear lamins, lamin A/C, which are the major components of the nuclear lamina, and form stable structures in the nuclear interior [8]. Although the nucleo-cytoskeletal connection through the LINC complex has been suggested to be crucial for many biological processes such as gene expression, cell motility, and disease pathogenesis [9,10], the detailed role of the LINC complex remains unclear.

Previous studies have suggested that nesprin-1 is also involved in cellular functions and diseases. For example, nesprin-1 knockdown by siRNA prevents the reorientation of ECs in response to cyclic stretching and causes a decrease in the cell migration speed [11]. Mutations in *SYNE1*, a gene encoding for nesprin-1, have been shown to be responsible for pathogenesis of diseases such as Emery–Dreifuss muscular dystrophy [12], cerebellar ataxia [13], and arthrogryposis [14]. In addition to these reports, the connection between the nucleus and F-actin through the LINC complex has been proposed to cause force transmission to the nucleus and directly regulate gene expression [15]. Therefore, an impaired connection between the nucleus and F-actin through nesprin-1 is considered to cause insufficient force transmission to the nucleus, which may lead to abnormal cellular functions and subsequent disease pathogenesis. However, the knowledge about the mechanical interaction between the nucleus and F-actin through nesprin-1 is limited.

In this study, we investigated the mechanical role of F-actin and nesprin-1 in force transmission to the nucleus by evaluating nucle-

* Corresponding author. Address: Department of Medical Engineering, Faculty of Health Science and Technology, Kawasaki University of Medical Welfare, 288 Matsushima, Kurashiki, Okayama 701-0193, Japan. Fax: +81 86 464 1109.
E-mail address: sakan@me.kawasaki-m.ac.jp (N. Sakamoto).
[1] Present address: Department of Medical Engineering, Faculty of Health Science and Technology, Kawasaki University of Medical Welfare, Okayama, Japan.

0006-291X/$ - see front matter © 2012 Elsevier Inc. All rights reserved.
http://dx.doi.org/10.1016/j.bbrc.2012.06.073

ar strain, an indicator of force transmission to the nucleus, from lateral cross-sectional images of nesprin-1 knocked-down ECs, subjected to uniaxial stretching. Nuclear strain in cells treated with cytochalasin D was also analyzed to determine the role of the entire F-actin structure on stretch-induced nuclear deformation.

2. Materials and methods

2.1. Cell culture

Human umbilical vein endothelial cells (HUVECs; Cascade Biologics, USA) were cultured in Medium 199 (Invitrogen, USA) containing 20% (v/v) heat-inactivated fetal bovine serum (FBS; SAFC Biosciences, USA), 10 ng/mL basic fibroblast growth factor (Austral Biologicals, USA), and 100 units/mL penicillin–streptomycin (Invitrogen). Cells at passages 4–6 were used in experiments. Prior to cell seeding, all cell culture dishes were coated with 0.1% bovine gelatin (Sigma–Aldrich, USA).

2.2. siRNA knockdown of nesprin-1 in ECs

For siRNA knockdown of nesprin-1, ECs were transfected with 100 nM siRNA targeting human nesprin-1 (SMARTpool siRNA Human *SYNE1*, Dharmacon, USA) using Dharmafect 1 transfection reagent (Dharmacon) according to the manufacturer's protocol. In brief, the cells were cultured for 24 h in Opti-MEM (Invitrogen) containing siRNA and for another 72 h in M199 medium without siRNA at 37 °C in a humidified atmosphere. The cells were then harvested and used for experiments. The siRNA oligonucleotide target sequences were as follows: CCAAACGGCUGGUGUGAUU, GAAGAGA CGUGGCGAUUGU, GCAAAGCCCUGGAUGAUAG, and GAAAUUGUCC CUAUUGAUU. The cells transfected with 100 nM control siRNA (Non-targeting siRNA Pool #2, Dharmacon) were used as controls to ensure that the decrease in nesprin-1 expression was related to a specific RNAi event. The nesprin-1 reduction level was assessed by Western blotting and immunofluorescence analysis.

2.3. Western blotting

ECs were cultured to confluence, washed three times with ice-cold PBS, and lysed in ice-cold Triton/NP-40 lysis buffer (50 mM Tris–Cl, 150 mM NaCl, 1 mM EDTA, 1% Triton X-100, 1% NP-40, 1 mM AEBSF, 800 nM aprotinin, 40 μM bestatin, 14 μM E-64, 20 μM leupeptin, 15 μM pepstatin A, 100 μM PMSF, pH 7.5) for 5 min. The lysates were centrifuged at 10,000 rpm for 10 min at 4 °C, following which the supernatants were collected and solubilized in sample buffer. Next, 30 μg of each protein sample was separated by SDS–PAGE with 10% polyacrylamide gel and transferred to a polyvinylidene difluoride (PVDF) membrane (GE Healthcare, UK). The membrane was blocked with 4% (w/v) Block Ace (Dainippon Pharma, Japan) for 1 h at room temperature, incubated with either rabbit anti-nesprin-1 antibody at a 1:2000 dilution (ab24742, Abcam, USA) or rabbit anti-GAPDH antibody at a 1:1000 dilution (ab37168, Abcam) overnight at 4 °C, and then probed with alkaline phosphatase-conjugated anti-rabbit secondary antibody at a 1:10,000 dilution (Santa Cruz Biotechnology, USA) for 1 h at room temperature. GAPDH was used as an internal control. Blots were developed using the DC protein assay kit (Bio-Rad Laboratories, USA).

2.4. Fluorescent staining

ECs cultured to confluence on a glass-bottom dish (AGC Techno Glass, Japan) were fixed with 4% paraformaldehyde, washed three times with PBS, permeabilized with 0.004% saponin for 10 min or 0.1% Triton X-100 for 5 min, and blocked with 1% (w/v) Block Ace for 1 h at room temperature. For membrane permeabilization, saponin was used when staining for nesprin-1 and Triton X-100 was used when staining for SUN1, SUN2, or lamin A/C. Next, the cells were incubated overnight at 4 °C with each of the following primary antibodies: rabbit anti-nesprin-1 at a 1:500 dilution, rabbit anti-SUN1 at a 1:100 dilution (HPA008461, Sigma–Aldrich), rabbit anti-SUN2 at a 1:100 dilution (HPA001209, Sigma–Aldrich), and mouse anti-lamin A/C at a 1:500 dilution (ab8984, Abcam). The cells were then washed three times with PBS and incubated with anti-rabbit or anti-mouse Alexa Fluor 488-conjugated secondary antibody at a 1:1000 dilution (Invitrogen) for 1 h at room temperature. To stain F-actin and nuclei, the cells were incubated with 150 nM Alexa Fluor 546-phalloidin (Invitrogen) for 20 min and 1 μg/ml DAPI (Invitrogen) for 5 min. Fluorescence images of the cells were obtained using an inverted confocal laser scanning microscope (FV1000, Olympus, Japan).

2.5. Cyclic stretching experiment

ECs were detached from a cell culture dish with 0.05% trypsin–EDTA, seeded at a concentration of 1.0×10^5 cells/mL on a fibronectin-coated polydimethylsiloxane (PDMS) membrane in a stretching chamber (Strex, Japan), and cultured to confluence at 37 °C in a humidified atmosphere for 24 h. The cells were then subjected to 10% uniaxial stretching at 0.5 Hz for 18 h using a stretching apparatus (STB-140, Strex) as described previously [11]. During the experiments, the stretching apparatus was maintained at 37 °C in an incubator.

2.6. Live cell imaging under stretching condition

ECs were seeded at a concentration of 5.0×10^4 cells/mL on a fibronectin-coated PDMS membrane in a stretching chamber and cultured at 37 °C in a humidified atmosphere for 24 h. Thirty minutes before the experiments, the cytoplasmic domains and nuclei of living cells were labeled with 10 μM Cell Tracker Red CMTPX (Invitrogen) and 1.6 μM Hoechst 33342 (Invitrogen), respectively. To evaluate the role of the entire intracellular F-actin structure in stretch-induced nuclear deformation, the cells were treated with 2 μM cytochalasin D (CytoD; Enzo Life Sciences, USA), a commonly used reagent for the inhibition of actin polymerization, for 30 min before the experiments. To maintain the appropriate pH at room atmosphere during the experiments, the medium was replaced with M199 medium with Hanks' salts (Invitrogen) containing 0.5% FBS and 100 units/mL penicillin–streptomycin.

For live cell imaging, a stretch application system consisting of a stretching chamber and a stretching apparatus (NS-600, Strex) was used (Fig. 1A). One end of the stretching chamber was firmly attached to a fixed frame, while the other end was held on a movable frame connected to a motor-driven shaft. The stretching apparatus was set on a cover glass attached to a stage of the inverted confocal laser scanning microscope equipped with a thermo-control system (Tokai hit, Japan). The friction between the cover glass and PDMS membrane of the stretching chamber was reduced by lubrication with 1% Triton X-100, which enabled the stretching chamber to be stretched smoothly.

Deformation behavior of the cells subjected to uniaxial stretching was observed performed as follows (Fig. 1B): a scanning line for obtaining lateral cross-sectional images of cells was set to be parallel to the direction of stretching and crossing the vicinity of the nuclear center in a horizontal cross-sectional image. Lateral cross-sectional images of the cells were obtained five times using a 60× objective lens (PLAPON, NA = 1.42, Olympus) in line-scanning mode at a pixel resolution of 100 nm/pixel. The time interval required for obtaining five images in lateral cross-section was

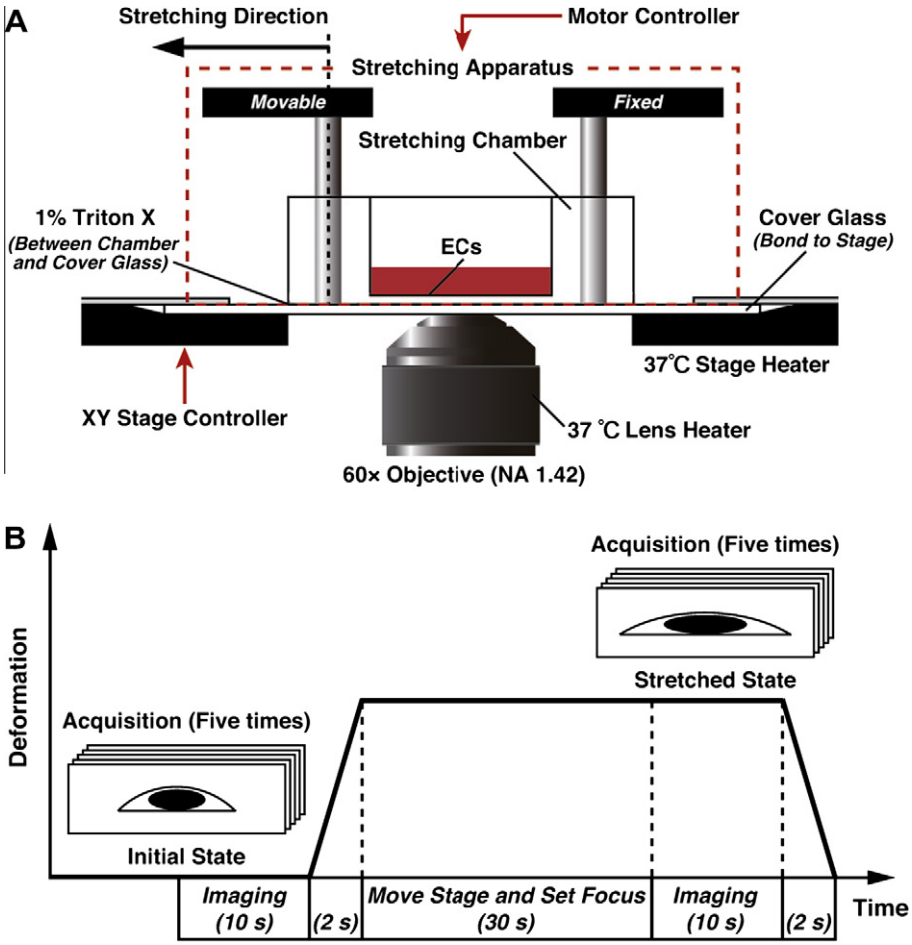

Fig. 1. Schematic diagram of the stretch application system. (A) The experimental setup for observing stretch-induced deformation of ECs. (B) Diagram of the imaging procedure.

approximately 10 s. An averaged image was then generated from the five obtained images using a Kalman filter. Next, the cells were subjected to 20% uniaxial stretching, and the stage was moved parallel to the direction of stretching followed by setting the focus on the cells. An averaged cross-sectional image of the deformed cells was obtained in the same way as that obtained before stretching the chamber.

2.7. Measurement of the horizontal nuclear length, nuclear height, and nuclear strain

The horizontal nuclear length, nuclear height, and nuclear strain in ECs subjected to uniaxial stretching were measured from lateral cross-sectional images of the cells using ImageJ 1.43u software (National Institutes of Health, USA). First, an 8-bit fluorescent image of the nucleus was converted to a binary image by the Otsu method [16], which is based on discriminant analysis and commonly used for binarization of gray-scale images. Second, the length between the left and right ends of the nucleus in the horizontal and vertical directions were measured. The measured horizontal and vertical lengths were defined as the horizontal nuclear length and height, respectively. Nuclear strain was calculated as $(L - L_o)/L_o$, where L_o is the horizontal nuclear length in cells in the initial state and L is the horizontal nuclear length in cells in the deformed state.

2.8. Data and statistical analysis

All data are presented as mean ± SD. All statistical analyses were performed using the Welch's *t*-test. Statistical significance was assumed for $p < 0.05$.

3. Results

3.1. Nesprin-1 knockdown in ECs

Representative results of Western blot analysis are shown in Fig. 2A. A single band of nesprin-1 in ECs was detected between marker bands of 279 and 500 kDa, consistent with results of previous studies [17,18]. Nesprin-1 expression in ECs transfected with siRNA targeting nesprin-1 (siNes1) significantly decreased compared with that in wild-type cells (Wt), whereas GAPDH expression as an internal control remained unchanged. Fluorescence microscopy showed that nesprin-1 localization to the nuclear envelope observed in Wt was depleted in the cells transfected with siNes1 (Fig. 2B). In addition, there were no changes in the nesprin-1 expression levels and localization in the control siRNA-transfected cells (siCon) compared with those in Wt. As a result of cyclic stretching experiments, Wt and siCon reoriented and elongated perpendicular to the stretching axis, whereas such morphological changes were suppressed in the cells transfected with siNes1 (Fig. 2C), as reported previously [11]. These results indicate that

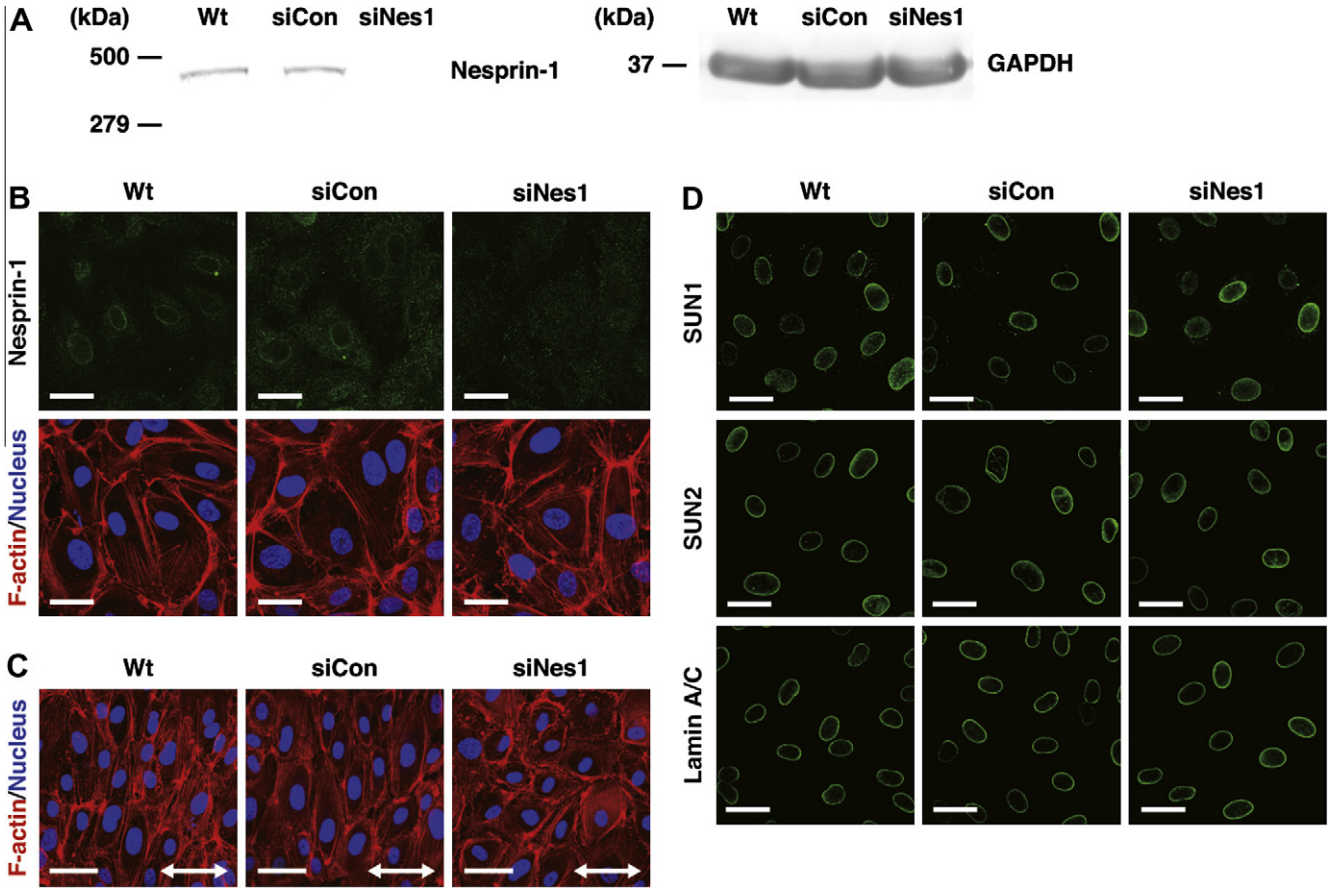

Fig. 2. Western blotting against nesprin-1 and fluorescence microscopy of F-actin, nuclei, and the LINC complex in ECs transfected with siRNA targeting nesprin-1. (A) Representative results of Western blotting against nesprin-1 and GAPDH in ECs. (B) Fluorescence images of nesprin-1 (green), F-actin (red), and nuclei (blue) in ECs under static conditions. (C) Fluorescence images of F-actin (red) and nuclei (blue) in ECs 18 h after exposure to 10% cyclic stretching at 0.5 Hz. (D) Fluorescence images of SUN1, SUN2, and lamin A/C in ECs under static conditions. Double-headed arrow represents the direction of stretching. Scale bar = 30 μM (B, D) and 50 μM (C). (For interpretation of the references to color in this figure legend, the reader is referred to the web version of this article.)

nesprin-1 expression in ECs was abolished by transfection of nesprin-1-specific siRNA. In contrast, fluorescence microscopy showed that SUN1, SUN2, and lamin A/C localized to the nuclear envelope even in nesprin-1 knocked-down cells (Fig. 2D), suggesting that nesprin-1 knockdown has no effect on localization of the other LINC complex proteins to the nuclear envelope.

3.2. Stretch-induced nuclear deformation in ECs

Representative lateral cross-sectional images of Wt, nesprin-1 knocked-down, and cytochalasin D-treated ECs before and after stretching are shown in Fig. 3A. Deformation behavior of the cells subjected to uniaxial stretching was successfully observed by confocal microscopy. In this study, deformation behavior of the cells was observed within 1 min. This observation time is about half of that reported in a previous study that observed deformation behavior of cells subjected to uniaxial stretching by confocal microscopy [19]. Therefore, active cell remodeling is considered to have little effect on obtained images. Wt subjected to uniaxial stretching showed nuclear deformation in the stretching direction as shown in Fig. 3A. Nuclear deformation in siCon was similar to that in Wt (data not shown). As a result of stretch application, nuclear deformation in the nesprin-1 knocked-down cells was greater than that in Wt, whereas the cytochalasin D-treated cells showed lesser nuclear deformation than Wt. In addition, the cytochalasin D-treated cells showed increased nuclear heights compared to Wt.

The horizontal nuclear lengths and nuclear heights in ECs before stretching are shown in Fig. 3B, C, respectively. Horizontal nuclear lengths in the nesprin-1 knocked-down cells and cytochalasin D-treated cells decreased significantly compared with those in Wt (Fig. 3B). Although there was no difference in the nuclear heights between Wt and nesprin-1 knocked-down cells, the nuclear heights in the cytochalasin D-treated cells increased significantly compared with that in Wt (Fig. 3C). This change in the nuclear height induced by cytochalasin D treatment was also reported in a previous study [20]. Transfection of control siRNA into cells caused no significant changes in the horizontal nuclear lengths and nuclear heights. These results indicate that the nuclear shape in the lateral cross-sectional images of the nesprin-1 knocked-down and cytochalasin D-treated cells was more circular than that in Wt.

Nuclear strain in ECs subjected to 20% uniaxial stretching is shown in Fig. 3D. Nuclear strain in the nesprin-1 knocked-down cells increased significantly compared with that in Wt. In contrast, nuclear strain in the cytochalasin D-treated cells decreased significantly compared with that in Wt, indicating that disruption of the intracellular F-actin structure by cytochalasin D treatment has a completely different effect on stretch-induced nuclear deformation from nesprin-1 knockdown by specific siRNA.

4. Discussion

Fluorescent microscopy revealed that nesprin-1 knockdown did not alter SUN1, SUN2, and lamin A/C localization to the nuclear envelope in ECs. These results are analogous to those reported in a previous study showing that SUN1, SUN2, and nesprin-2

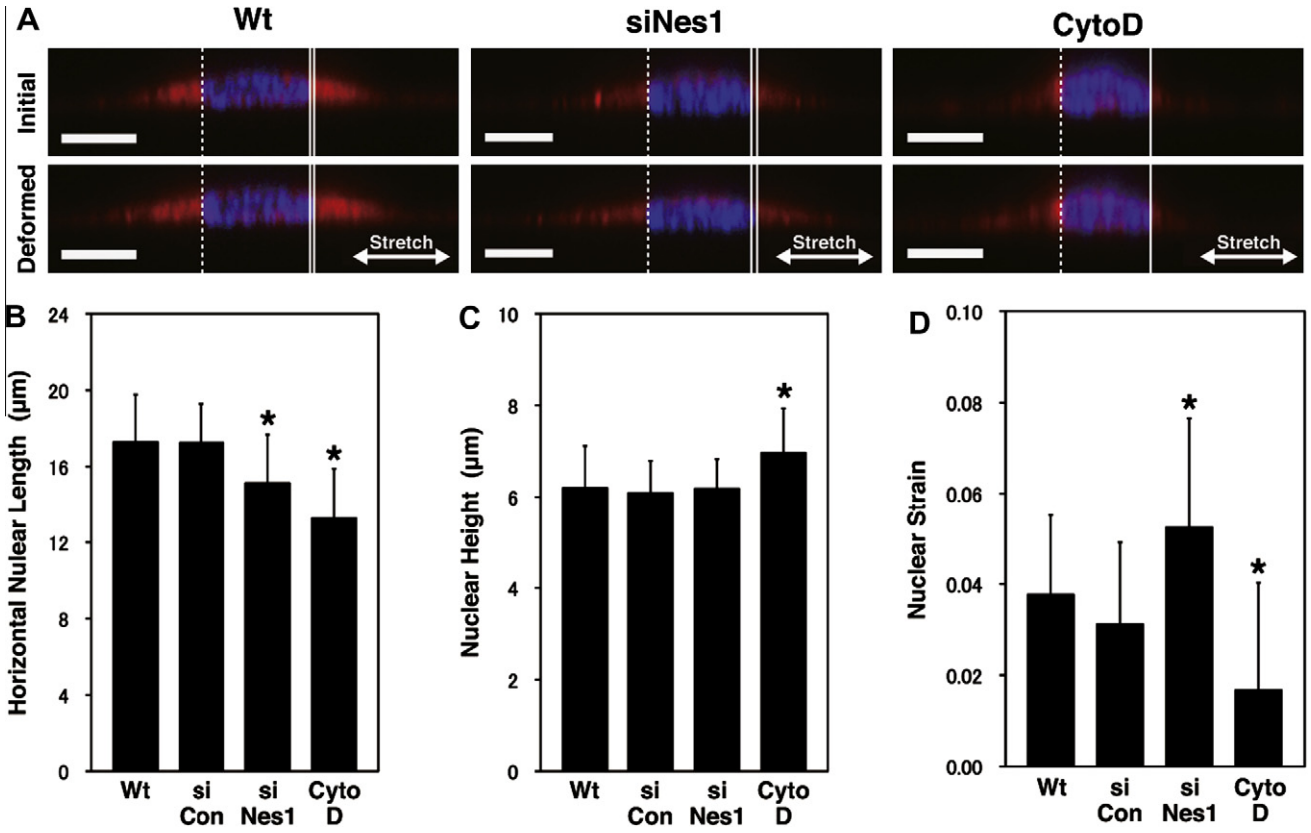

Fig. 3. The initial nuclear shape and strain in ECs subjected to 20% uniaxial stretching. (A) Representative images of cells before and after stretching. The left ends of nuclei in cells in the initial state and deformed state are fitted (dashed line). The interval between the two solid lines drawn on the right ends of nuclei in cells in the initial state and deformed state represents the magnitude of nuclear deformation. (B) The horizontal nuclear lengths and (C) nuclear heights in cells in the initial state. (D) Nuclear strain in cells subjected to 20% uniaxial stretching. Double-headed arrow represents the direction of stretching. Scale bar = 10 μM. Wt: $n = 20$, siCon: $n = 21$, siNes1: $n = 21$, CytoD: $n = 20$. $^{*}p < 0.05$ vs. Wt.

localization to the nuclear envelope was not altered in mouse embryo fibroblasts (MEFs) from mice lacking the lamin A/C gene (*LMNA*) [21]. SUN1/2 are transmembrane proteins existing in the perinuclear space, which penetrate the nuclear envelope and bind to lamin A/C in the nuclear interior [6,7]. Therefore, SUN1/2 are considered to be fixed to the nuclear envelope even in nesprin-1 knocked-down cells or those lacking lamin A/C, resulting in SUN1/2 and lamin A/C localization to the nuclear envelope in nesprin-1 knocked-down cells and SUN1/2 and nesprin-2 localization to the nuclear envelope in cells lacking lamin A/C. In addition, there were no nuclei with abnormal shapes in nesprin-1 knocked-down cells, which are typically observed in cells lacking *LMNA* [22,23]. This suggests that nesprin-1 is not a structural component of the nucleus, but is rather a coupling element that mediates interactions between F-actin and the nucleus.

In this study, nuclear strain in ECs subjected to uniaxial stretching was evaluated to investigate force transmission to the nucleus through F-actin bound to nesprin-1. Contrary to our expectations, nuclear strain in the nesprin-1 knocked-down cells increased significantly compared with that in Wt. However, consistent with our expectations, nuclear strain in the cytochalasin D-treated cells decreased significantly compared with that in Wt. These results cannot be explained by a simple hypothesis that the nucleus is deformed only by the tension generated by F-actin bound to the nucleus through the LINC complex in cells subjected to uniaxial stretching.

To explain these findings, we propose a model that describes mechanical interactions between F-actin and the nucleus in cells subjected to uniaxial stretching (Fig. 4). It can be assumed that cells have F-actin structures of basal stress fibers, nesprin-1-binding F-actin, and the actin cortical layer beneath the cell membrane or a perinuclear actin cap [24]. The top row of Fig. 4 represents the intracellular F-actin structures and the nucleus in cells under static conditions. Wt and siCon have all these F-actin structures, whereas F-actin bound to nesprin-1 is depleted in nesprin-1 knocked-down cells, and all the F-actin structures are disrupted in cytochalasin D-treated cells. Because it has not been reported that basal stress fibers are involved in regulation of nuclear shape, only F-actin bound to nesprin-1 and the actin cortical layer are considered to be involved in mechanical interaction with the nucleus.

The nuclei in Wt are considered to be subjected to tensile force in the horizontal direction exerted on the nucleus by F-actin bound to nesprin-1 and compressive force in the vertical direction exerted on the nucleus by the actin cortical layer, which may sustainably deform the nucleus in cells under static condition [26], as described in the middle row of Fig. 4. In contrast, the nuclei of nesprin-1 knocked-down cells are considered to be released from the tension by F-actin bound to the nuclei, thereby increasing allowance for nuclear deformation. Similarly, the nuclei of cytochalasin D-treated cells are considered to be released from the tension in the horizontal direction and compression in the vertical direction by disruption of the entire F-actin structure, which may further increase allowance for nuclear deformation.

Based on these assumptions, it is possible that the nucleus with an increased allowance for deformation is compressed by the actin cortical layer in nesprin-1 knocked-down cells subjected to uniaxial stretching, as described in the bottom row of Fig. 4, resulting in increased nuclear strain with that in Wt. In contrast, despite an increased allowance for nuclear deformation, nuclear strain in

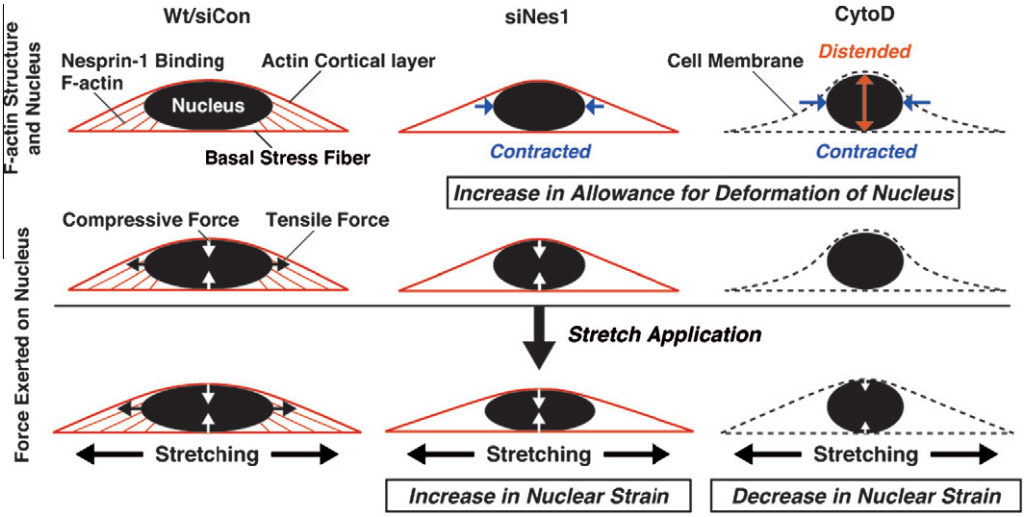

Fig. 4. Mechanical model of interactions between F-actin and nuclei in cells subjected to uniaxial stretching. Top images represent F-actin structures and nuclei in cells before stretching. Middle and bottom images represent tensile force exerted on the nucleus by F-actin bound to nesprin-1 and compressive force exerted on the nucleus by the actin cortical layer of cells before and after stretching, respectively.

cytochalasin D-treated cells was significantly decreased compared with that in Wt, which could have been caused by exertion of little tension and little compression of the nucleus by disrupted F-actin.

Based on these perspectives, the results of this study suggest that F-actin bound to the nucleus through nesprin-1 causes sustainable force transmission to the nucleus even in cells under static conditions. This supports the previously proposed idea that force transmission to the nucleus regulates gene expression by causing conformational changes in the DNA structure and by regulating nuclear transport [15]. Although some previous studies have suggested that defective nucleo-cytoskeletal connections impair the activation of mechanosensitive genes such as *Iex-1* and *Egr-1* [22,25], whether impaired gene expression is caused by a loss of direct force transmission to the nucleus or a defect in biological signaling induced by mechanical stimuli remains unclear. Thus, further investigation is needed to determine whether force transmission to the nucleus directly regulates gene expression.

Acknowledgments

This study was supported in part by Grants-in-Aid for Scientific Research from the Ministry of Education, Culture, Sports, Science and Technology (MEXT) of Japan (Nos. 20001007 and 23650250).

References

[1] D.E. Discher, P. Janmey, Y.L. Wang, Tissue cells feel and respond to the stiffness of their substrate, Science 310 (2005) 1139–1143.
[2] R.M. Mège, J. Gavard, M. Lambert, Regulation of cell–cell junctions by the cytoskeleton, Curr. Opin. Cell Biol. 18 (2006) 541–548.
[3] J. Renkawitz, M. Sixt, Mechanisms of force generation and force transmission during interstitial leukocyte migration, EMBO Rep. 11 (2010) 744–750.
[4] G. Civelekoglu-Scholey, J.M. Scholey, Mitotic force generators and chromosome segregation, Cell. Mol. Life Sci. 67 (2010) 2231–2250.
[5] M. Crisp, Q. Liu, K. Roux, J.B. Rattner, C. Shanahan, B. Burke, P.D. Stahl, D. Hodzic, Coupling of the nucleus and cytoplasm: role of the LINC complex, J. Cell Biol. 172 (2006) 41–53.
[6] D.T. Warren, Q. Zhang, P.L. Weissberg, C.M. Shanahan, Nesprins: intracellular scaffolds that maintain cell architecture and coordinate cell function?, Expert Rev Mol. Med. 7 (2005) 1–15.
[7] J.A. Mellad, D.T. Warren, C.M. Shanahan, Nesprins LINC the nucleus and cytoskeleton, Curr. Opin. Cell Biol. 23 (2011) 47–54.
[8] K.N. Dahl, A.J. Ribeiro, J. Lammerding, Nuclear shape, mechanics, and mechanotransduction, Circ. Res. 102 (2008) 1307–1318.
[9] A. Méjat, T. Misteli, LINC complexes in health and disease, Nucleus 1 (2010) 40–52.
[10] M.L. Lombardi, J. Lammerding, Keeping the LINC: the importance of nucleocytoskeletal coupling in intracellular force transmission and cellular function, Biochem. Soc. Trans. 39 (2011) 1729–1734.
[11] T.J. Chancellor, J. Lee, C.K. Thodeti, T. Lele, Actomyosin tension exerted on the nucleus through nesprin-1 connections influences endothelial cell adhesion, migration, and cyclic strain-induced reorientation, Biophys. J. 99 (2010) 115–123.
[12] Q. Zhang, C. Bethmann, N.F. Worth, J.D. Davies, C. Wasner, A. Feuer, C.D. Ragnauth, Q. Yi, J.A. Mellad, D.T. Warren, M.A. Wheeler, J.A. Ellis, J.N. Skepper, M. Vorgerd, B. Schlotter-Weigel, P.L. Weissberg, R.G. Roberts, M. Wehnert, C.M. Shanahan, Nesprin-1 and -2 are involved in the pathogenesis of Emery Dreifuss muscular dystrophy and are critical for nuclear envelope integrity, Hum. Mol. Genet. 16 (2007) 2816–2833.
[13] F. Gros-Louis, N. Dupré, P. Dion, M.A. Fox, S. Laurent, S. Verreault, J.R. Sanes, J.P. Bouchard, G.A. Rouleau, Mutations in SYNE1 lead to a newly discovered form of autosomal recessive cerebellar ataxia, Nat. Genet. 39 (2007) 80–85.
[14] R. Attali, N. Warwar, A. Israel, I. Gurt, E. McNally, M. Puckelwartz, B. Glick, Y. Nevo, Z. Ben-Neriah, J. Melki, Mutation of SYNE-1, encoding an essential component of the nuclear lamina, is responsible for autosomal recessive arthrogryposis, Hum. Mol. Genet. 18 (2009) 3462–3469.
[15] N. Wang, J.D. Tytell, D.E. Ingber, Mechanotransduction at a distance. Mechanically coupling the extracellular matrix with the nucleus, Nat. Rev. Mol. Cell Biol. 10 (2009) 75–82.
[16] N. Otsu, A threshold selection method from gray-level histograms, IEEE Trans. Syst. Man Cybern. 9 (1979) 62–66.
[17] Q. Zhang, J.N. Skepper, F. Yang, J.D. Davies, L. Hegyi, R.G. Roberts, P.L. Weissberg, J.A. Ellis, C.M. Shanahan, Nesprins: a novel family of spectrin-repeat-containing proteins that localize to the nuclear membrane in multiple tissues, J. Cell Sci. 114 (2002) 4485–4498.
[18] V.C. Padmakumar, S. Abraham, S. Braune, A.A. Noegel, B. Tunggal, I. Karakesisoglou, E. Korenbaum, Enaptin, a giant actin-binding protein, is an element of the nuclear membrane and the actin cytoskeleton, Exp. Cell Res. 295 (2004) 330–339.
[19] N. Caille, Y. Tardy, J.J. Meister, Assessment of strain field in endothelial cells subjected to uniaxial deformation of their substrate, Ann. Biomed. Eng. 26 (1998) 409–416.
[20] F. Guilak, Compression-induced changes in the shape and volume of the chondrocyte nucleus, J. Biomech. 28 (1995) 1529–1541.
[21] C. Ostlund, E.S. Folker, J.C. Choi, E.R. Gomes, C.G. Gundersen, H.J. Worman, Dynamics and molecular interactions of linker of nucleoskeleton and cytoskeleton (LINC) complex proteins, J. Cell Sci. 122 (2009) 4099–4108.
[22] J. Lammerding, P.C. Schulze, T. Takahashi, S. Kozlov, T. Sullivan, R.D. Kamm, C.L. Stewart, R.T. Lee, Lamin A/C deficiency causes defective nuclear mechanics and mechanotransduction, J. Clin. Invest. 113 (2004) 370–378.
[23] T. Dechat, K. Pfleghaar, K. Sengupta, T. Shimi, D.K. Shumaker, L. Solimando, R.D. Goldman, Nuclear lamins: major factors in the structural organization and function of the nucleus and chromatin, Genes Dev. 22 (2008) 832–853.
[24] S.B. Khatau, C.M. Hale, P.J. Stewart-Hutchinson, M.S. Patel, C.L. Stewart, P.C. Searson, D. Hodzic, D. Wirtz, A perinuclear actin cap regulates nuclear shape, Proc. Natl. Acad. Sci. USA 106 (2010) 19017–19022.
[25] J. Lammerding, J. Hsiao, P.C. Schulze, S. Kozlov, C.L. Stewart, R.T. Lee, Abnormal nuclear shape and impaired mechanotransduction in emerin-deficient cells, J. Cell Biol. 170 (2005) 781–791.
[26] S. Deguchi, K. Maeda, T. Ohashi, M. Sato, Flow-induced harding of endothelial nucleus as an intracellular stress-bearing organelle, J. Biomech. 38 (2005) 1751–1759.